Effect of Geometric Structure of Flow Promoting Agents on the Flow Properties of Pharmaceutical Powder Mixture

Kotoe Machida Ohta,[1,4] Masayoshi Fuji,[2] and Masatoshi Chikazawa[3]

Received November 30, 2002; accepted January 22, 2003

Purpose. The object of this work was to investigate the mechanism of how the surface geometric structure of flow agents affects on the flowability of pharmaceutical powder mixtures.

Methods. Nonporous and porous silicas were mixed with directly compressible fillers as flow promoting agents. The geometric structure of flow agents was investigated by gas adsorption and laser diffraction analysis. Flowability was evaluated with Carr's index measurement. Adhesion force between fillers and flow agents was determined using atomic force microscopy.

Results. Flowability was improved with the addition of both nonporous and porous flow agents. In the case of nonporous flow agents, effect to promote flowability decreased with the increase of particle diameter, whereas porous flow agents highly improved flowability independent of particle diameter. Atomic force microscopy measurement found that the adhesion force between a porous agent and filler was smaller than that between a nonporous agent and filler.

Conclusions. Enhancement of flowability varies depending on the geometric structure of flow agents. Porous flow agents improve flow properties more than nonporous agents, because porosity is highly contributed to reduction of adhesion force between particles.

KEY WORDS: flowability; flow agent; geometric structure; adhesion force; atomic force microscope.

INTRODUCTION

Flow property is one of the important characteristics of pharmaceutical powder mixtures because it influences content and weight uniformity at the process of mixing, tableting, and capsulation. For the purpose of improving the flowability of particles, flow agents, such as talc, colloidal silicas, and magnesium stearate (1–3), are widely incorporated in solid dosage forms.

The field of flow agent is treated by many authors. Chowhan and Yang (4) reported that powder mixtures comprising up to 1% colloidal silica generally resulted in the increase of flow rate. Lubner and Ricciardiello (5) verified that addition of colloidal silicas is effective only when used at optimal concentration ranges. Otsuka (6) observed that the adhesive force was remarkably reduced in the presence of ultra fine particles and the addition of adequate amount of flow agent led to an increase of powder fluidity.

However, most of these studies are focused on the optimal concentration range of flow agent but the mechanism to improve of the flowability or effect of geometric structure of flow agent has not been investigated qualitatively. Sindel and Zimmermann (7) considered that flow properties were determined by adhesion force acting between particles and established the technique to measure the force between individual lactose particles, but the effect of surface geometric structure on the flowability was not studied sufficiently.

The main object of this work is to investigate the effect of geometric structure of flow agent on flowability and to clarify the mechanism of enhancing flowability. Six nonporous and porous silicas were used as flow promoting agents and flowability was evaluated by Carr's index. Adhesion force between particles was measured by atomic force microscope (AFM). The relationship between flowability and geometric structure was analyzed, being related to the adhesion force between particles.

MATERIALS AND METHODS

Materials

The following silicas were purchased from commercial suppliers and used as received: Aerosil 200 and Aerosil 50 (Nippon Aerosil Co., Ltd., Tokyo, Japan); SO-C1 and SO-C5 (Admatechs Co., Ltd., Aichi, Japan); CARPLEX CS-5 (Shionogi & Co., Ltd., Osaka, Japan); and Adsolider 101 (Freund Industrial Co., Ltd., Tokyo, Japan). Tablettose 80 (MEGGLE GmbH, Wasserburg, Germany) and Avicel PH101 (Asahi Kasei Corporation, Osaka, Japan) were used as directly compressible fillers.

Methods

Sample Preparation

Tablettose 80 and Avicel PH101 were premixed at the ratio of 7:3 in drum mixture (Nisida Chemical Equipment Mfg. Ltd, Osaka, Japan) for 30 min and screened with a 1-mm mesh sieve. Sieved mixture was poured into silica particles that were screened with a 500-μm mesh sieve and mixed in a Turbula mixer T2C (Willy A.Bachofen AG Maschinenfabrik, Bassel, Switzerland) for 20 min. The total amount of powder mixture was fixed at 350 g and prepared samples were stored at 18–26°C and 30–60% relative humidity.

Determination of Surface Geometric Structure of Silica and Fillers

Specific surface area and porosity were evaluated by gas adsorption method. Adsorption isotherms of nitrogen at –196°C were measured by FlowSorb 2300 and TriStar 3000 (Shimadzu Corporation, Kyoto, Japan). The general value of $\sigma_{N2} = 0.162\text{nm}^2$ was taken as the cross sectional area of a nitrogen molecule. The specific surface areas S_{N2} of the samples were calculated by the BET method and the pore size

[1] Department of Pharmaceutical Research, Nippon Boehringer Ingelheim Co., Ltd., 3-10-1, Yato, Kawanishi, Hyogo, Japan.
[2] Ceramics Research Laboratory, Nagoya Institute of Technology, 10-6-29 Asahigaoka Tajimi, Gifu, Japan.
[3] Department of Applied Chemistry, Graduate School of Engineering, Tokyo Metropolitan University, 1-1 Minami-ohsawa, Hachioji, Tokyo, Japan.
[4] To whom correspondence should be addressed. (mailing address: 3-10-1, Yato, kawanishi, Hyogo 666-0193, Japan. Tel: +81-(0)72-790-2320; Fax: +81-(0)72-792-7961; E-mail: ohta@boehringer-ingelheim.co.jp)

0724-8741/03/0500-0804/0 © 2003 Plenum Publishing Corporation

distributions were figured out by the BJH Desorption Pore Distribution method (8).

Laser diffraction analysis was used for the determination of particle size distribution. The particle size of fillers was measured in gas phase mode and the size of silicas was conducted in liquid phase mode. In advance of liquid mode measurement, silica particles were dispersed into distilled water with adding Polysorbate 80 as surfactant. Prepared dispersion was exposed to super ultrasonic for 10 min to avoid the aggregation of single particles and these samples were set to diffraction analyzer Heros & Rodos (Sympatec GmbH, Clausthal-Zellerfeld, Germany). Particle size of Aerosil 50 and Aerosil 200 is too small and below detection limit, therefore these values are quoted from Aerosil catalogues.

Evaluation of Flowability

Flowability was expressed as Carr's index. This total index was obtained from particle size uniformity, repose angle, compressibility and spatula angle. Particle size uniformity was calculated from undersize distribution of initial filler mixture and the value 4.3 was used for all the samples. The other indexes were measured by Powder Characteristics Tester (Hosokawamicron Corporation, Osaka, Japan).

Adhesion Force Measurement Using AFM

There had been several techniques to measure the adhesion force between particles such as centrifugal and impact separation methods. However, all of these methods are restricted to be applied only on bigger sample quantities and measurement on an individual particle had turned out to be very difficult until recent technological development of adhesion force measurement devices (9–11). For instance, Shimada *et al.* (9) recently developed a new apparatus that can measure adhesion force and monitor the behavior of individual particles simultaneously.

AFM is one of these measurement devices (12). The head unit of AFM (Fig. 1) consists of a cantilever that works as a probe and piezo unit. Piezo unit controls the displacement of substrate and force measurement is conducted between a probe and substrate in "force curve" mode. In this operating mode, the substrate displacement was controlled by the piezo movement, and adhesion force was converted from the deflection of a cantilever and its spring constant. In this study, all the measurements were obtained by AFM SPI300 (Seiko Instruments Inc., Chiba, Japan) and analyzed using a SPA3700 system.

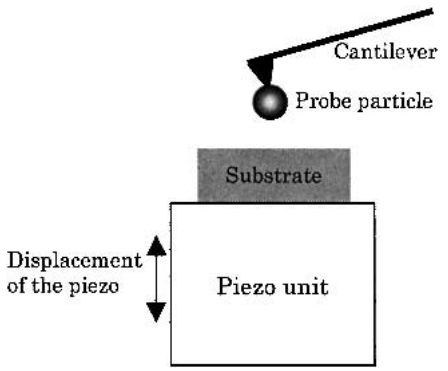

Fig. 1. Illustration of head unit of atomic force microscope. A probe silica particle was glued to the top of cantilever by epoxy resin and a substrate is a filler tablet. Adhesion force was measured between probe silica and a filler tablet.

Adhesion force was measured between a silica particle and a filler tablet. A filler tablet was prepared by single-punch tablet press (Korsch AG, Berlin, Germany) at 1000 kg tableting force. A powder mixture (340 mg) was compacted into flat-faced tablets with a diameter of 10 mm without any lubricant. A silica particle was fixed on the top of cantilever using epoxy resin (1). Before the measurement, the diameter of a particle was confirmed by optical microscope and an obtained force f was normalized by the following equation.

$$F = \frac{f}{R} \tag{1}$$

where R is the curvature radius of a silica particle attached to the cantilever. Adhesive force measurement was conducted under 30% relative humidity to avoid the significant influence of liquid bridge adhesion force (13,14).

RESULTS AND DISCUSSION

Surface Geometric Structure

Geometric structure of silica particles is summarized in Table I. Hysterisis loop in desorption isotherm of nitrogen was observed only for Adsolider 101 and CARPLEX CS-5. Hysterisis loop is a characteristic of porous structure (15) and did not appear in other four silicas. Figure 2 shows pore size distribution of Adsolider 101 and CARPLEX CS-5. In Table I, surface roughness G was listed by calculated according to the equation given below (15,16),

$$G = \frac{S_{N2}}{A} \tag{2}$$

$$A = \frac{6}{\rho} \sum_{k=1}^{27} \frac{D_k}{L_k} \tag{3}$$

S_{N2} is specific surface area obtained from gas adsorption. A is specific surface area calculated, assuming the ideal case that particles are equal-sized and perfectly spherical in shape. Here, ρ is the true density and D_k is a particle size frequency at each section. Particle size distribution was divided into 27 sections and L_k is the mean particle size in each section. $G = 1$ means that the sample has a unique size and smooth surface structure. A large G value demonstrates that the sample has wider size distribution and rougher surface structure.

Table I shows that four samples are nonporous and the other two samples are porous particles, as expected from the manufacturing process. Particle size of nonporous silica is in the order of Aerosil 200 < Aerosil 50 < SO-C1 < SO-C5 and particle size of SO-C5 is almost the same as Adsolider 101, which has a porous structure. Specific surface area of nonporous samples decreased in inverse proportion to particle diameter because nonporous silica has no internal surface area whereas porous samples that included large internal surface area revealed high surface areas.

Differences in surface structure also appeared in surface roughness. The value of surface roughness G is extremely high on porous samples, whereas it is near to 1.0 in the case of

Table I. Surface Geometric Structure of Silica Samples

	Manufacturing process	Mean particle size (μm)	Specific surface area (m^2/g)	Pore size diameter (nm)	Pore volume (mL/g)	True density (g/mL)	Surface roughness G
Aerosil200	Gas phase	0.012	194	Nonporous	Nonporous	2.2	0.85
Aerosil50	Gas phase	0.030	53.2	Nonporous	Nonporous	2.2	0.59
SO-C1	Gas phase	0.42	13.6	Nonporous	Nonporous	2.2	1.8
SO-C5	Gas phase	1.0	3.62	Nonporous	Nonporous	2.2	1.1
Adsolider 101	Liquid phase	0.97	289	19	1.6	2.2	69
CS-5	Liquid phase	2.0	136	31	0.81	2.0	65

Note: Manufacturing process and true density are quoted from each silica catalogs. Surface roughness was calculated from Eqs. (2) and (3). Mean diameter of Aerosil 50 and Aerosil 200 is quoted from Aerosil catalog and used for calculation for surface roughness.

nonporous silica. In other words, nonporous silica has a smooth surface and porous silica holds much rougher surface structures.

Flowability

Figure 3a depicts the Carr's index of series of nonporous silicas. Index value of initial filler mixture without any flow agent is 66.0, and it increased in accordance with the addition of flow agent to show a local maximum value. In the case of nonporous silicas, the enhancement of flowability reduced with the increase of particle diameter, while optimum concentration shifted to higher ratio with the increase of diameter. For example, when focused on the local maximum value, Aerosil 200, with a diameter of 12 nm, showed maximum value 75.0 at 0.1wt%, but it deceased to 72.0 at 3 to 5wt% with the addition of SO-C5, which are 1.0 μm in diameter.

However, different tendency was obtained in the case of porous silica, as seen in Fig. 3b. Flowability was highly improved and showed maximum value, independent of particle size. For instance, particle diameter of CARPLEX CS-5 is as twice as Adsolider 101, but local maximum values of these two samples were almost the same at the same concentration. Considering the effect of porosity, Adsolider 101, which is a porous structure and has similar diameter to nonporous SO-C5, showed higher ability to enhance the flowability compared with SO-C5. This result indicated flowability is strongly affected by the porosity and rougher surface structure is effective as flow promoting agents.

According to these results, effect of surface geometric structure can be summarized as follows:

1. In the case of nonporous silicas, enhancement of flowability reduces with the increase of particle diameter.
2. In the case of porous silicas, flowability is highly improved, independent of particle size.

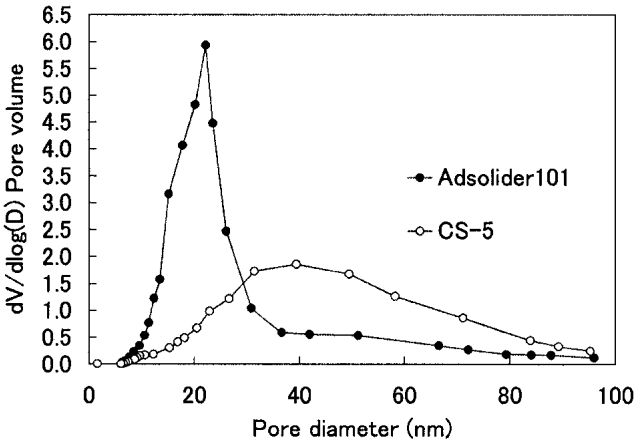

Fig. 2. BJH Desorption Pore Distribution of porous silicas. Hysterisis loop in desorption isotherm was observed for Adsolider 101 and CARPLEX CS-5. Hysterisis loop is a characteristic of porous structure and indicates that only these two silicas involve pore in particle structure.

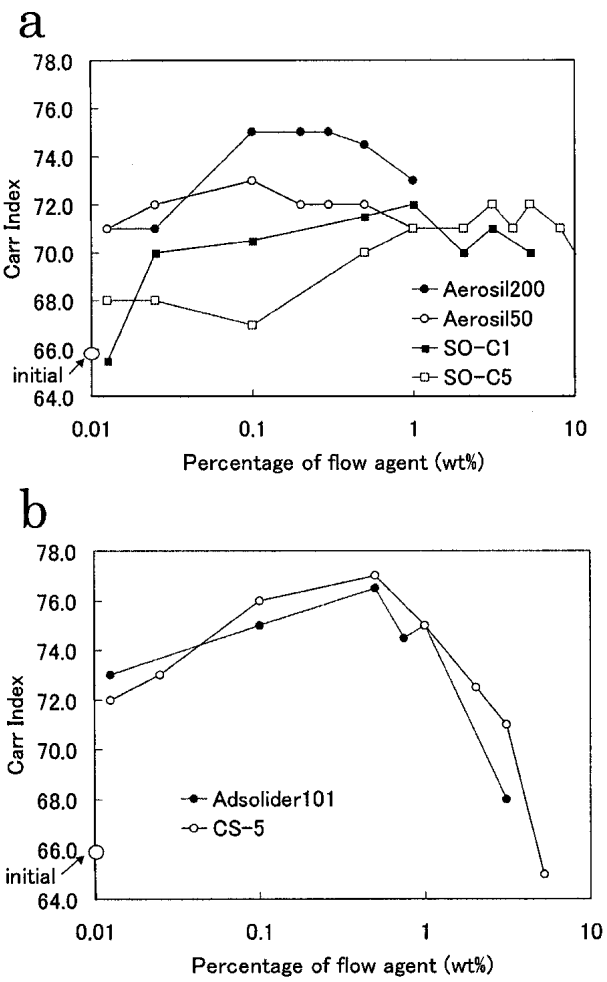

Fig. 3. (a) Carr's index of series of nonporous silica series. (b) Carr's index of series of porous silicas.

3. If particle diameter is the same, porous silica is more effective to enhance the flowability than nonporous silica.

AFM

Relationship between the surface geometric structure and flowability was shown but the mechanism how surface structure effects on the flowability remains unsolved. Otsuka (6) investigated flowability and adhesion force between individual particles and verified that flowability was improved with the reduction of adhesion force. Based on this concept, effect of surface structure on adhesion force and how it affects on flowability were evaluated.

Adhesion force was measured using AFM. Adsolider 101 and SO-C5 were chosen as probe particles, since these samples have almost the same particle size and different surface geometric structure. Before measurement, topography images of filler tablets were acquired in noncontact mode. Force measurement was conducted only after surface clear image was taken and adhesion force was obtained more than 20 individual sites.

Adhesion force f is normalized by Eq. (1) and plotted in Fig. 4 as cumulative distribution of normalized adhesion force. The 50% medium value was figured out and listed in Table II. Adhesion force between porous Adsolider 101 and filler is smaller than that between nonporous SO-C5 and filler as to the same fillers. This result indicated that porous structure is effective to reduce the adhesion force. Mizes *et al.* (17) analyzed the adhesion force and reported that adhesion force is controlled by the surface roughness. Table I shows that porous silica includes much more surface roughness compared with nonporous silica. Consequently, it is considered that roughness is contributed to the reduction of adhesion force between particles, and leads to enhancement of flowability.

The mechanism how surface roughness reduces adhesion force has been discussed mainly from two viewpoints (18–22). One is the effect of contact area and the other is effect of surface curvature at the contact points. Cooper *et al.* (18) reported that the contact areas varied considerably depending on the degree of surface roughness and that microscale roughness played a controlling role in particle adhesion. Schaefer *et al.* (19) studied adhesion force between particles and explained the disparity between theoretical and experimental values by estimating radius of the contact asperity.

Regarding to silica particles, both factors can be considered to determine the adhesion force. Surface roughness of porous Adsolider 101 leads to reduce the contact area compared with nonporous SO-C5, which has a rather smooth surface structure. This effect can be further investigated if tested another porous silica, which has different porous structure from Adsolider 101.

The latter factor also should be worked to reduce the adhesion force. Adhesion force between a silica particle and filler can be expressed by Derjaguin approximation (23) given by the following:

$$F = 2\pi W \left(\frac{R_s R_f}{R_s + R_f} \right) \tag{4}$$

Where R_s and R_f are the radius of surface curvature at the point of contact for a silica and filler particle, respectively. W is the work of adhesion. In this study, R_f can be considered to be constant regarding to the same filler, therefore adhesion force is determined by R_s. In the case of nonporous silica, R_s increases in proportion to particle diameter, because nonporous silica has smooth surface structure and is almost near to true spherical shape. Therefore, adhesion force increases with particle diameter and results in the reduction of flowability. When it comes to porous silica, surface roughness reduces Rs and flowability is highly improved independent of particle diameter. This mechanism is illustrated in Fig. 5.

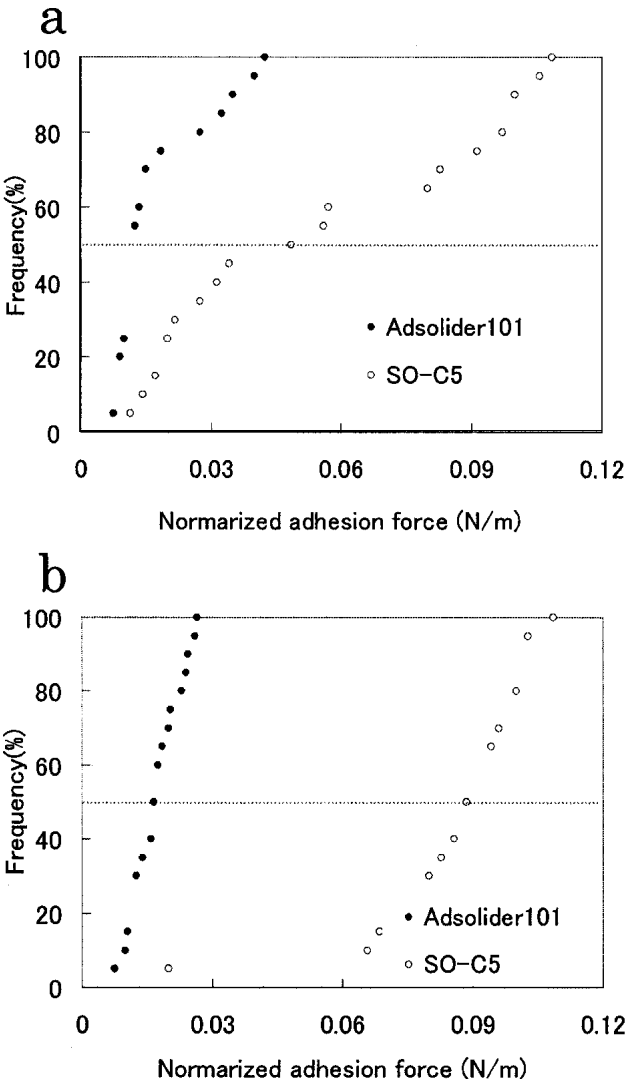

Fig. 4. Adhesion force measured by atomic force microscope between a silica particle and (a) Avicel PH101 tablet, (b) Tablettose80 tablet. This graph represents the cumulative of normalized adhesion force expressed in percentage.

Table II. Adhesion Force between a Silica and Filler Tablet

	Filler table	Median value (N/m)
SO-C5	Tablettose80	8.9×10^{-2}
	Avicel PH101	4.9×10^{-2}
Adsolider101	Tablettose80	1.7×10^{-2}
	Avicel PH101	1.2×10^{-2}

Note: Obtained adhesion force was normalized by Eq. (1).

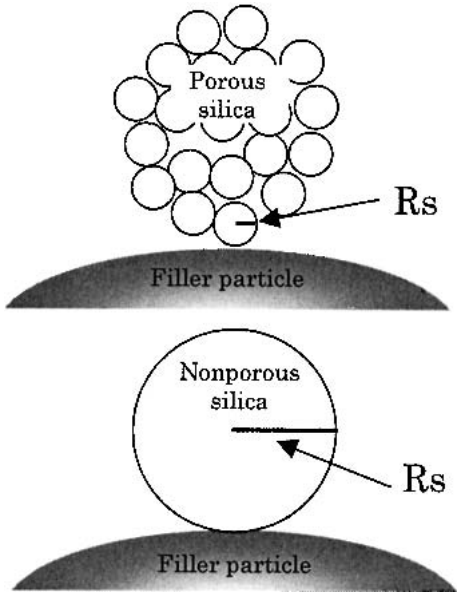

Fig. 5. Adhesion force was determined by the particle radius of curvature R_s at the contact point. Surface roughness of porous silica is contributed to reduce the adhesion force, whereas nonporous silica shows high adhesion force because of smooth surface structure.

Another interesting finding in Fig. 4 and Table II is that adhesion force works with Tablettose 80 is approximately twice as large as that with Avicel PH101.

This difference could be explained in terms of higher surface energy of Tablettose 80 than that of Avicel PH101 because it would change the work of adhesion between silica and fillers. However, this hypothesis is denied by the fact that there is only a slight difference in surface energy, which was verified by contact angle measurement. (24)

Another inference is influence of surface morphology, which was already discussed above. Table III shows the mean particle size and specific surface area of fillers. Mean particle size of Avicel PH101 is slightly smaller than that of Tablettose80, though specific surface area is much larger than that of Tablettose80. Large surface area and small diameter indicated that Avicel PH101 has rougher surface compared to Tablttose80. Therefore, it is considered that the degree of surface roughness altered contact area and radius of surface curvature R_f in equation (4) and arisen the reduction of the adhesion force.

From adhesion measurement, it can be concluded that porosity of silica plays an important role to reduce the adhesion force and it leads to the enhancement of flowability more than nonporous structure. Additionally, higher adhesion force observed between silica and Tablettose 80 can be explained from the aspect of difference of surface morphology.

CONCLUSION

Nonporous and porous silica was mixed with pharmaceutical filler mixture and flowability was evaluated. Enhancement of flowability is reduced with the increase of particle diameter of nonporous silica. Although porous flow agents improve flow properties independent of particle size. AFM force measurement verified that adhesion force between porous silica and filler is smaller than that between a nonporous silica and filler. These results indicated that porous structure is highly contributed to reduction of adhesion force because of rougher surface structure. Both reduction of contact area and smaller radius of curvature at the point of contact account for the decrease of adhesion force and lead to the improvement of flowability. In addition, it was also seen that adhesion force was alerted because of the different morphology of filler surfaces.

Table III. Mean Particle Size and Specific Surface Area of Fillers

	Mean particle size (μm)	Specific surface area (m^2/g)
Tablettose80	83	0.41
Avicel PH101	62	1.11

REFERENCES

1. M. S. H. Hussain, P. York, and P. Timmins. A study of the formation of magnesium stearate film on sodium chloride using energy-dispersive X-ray analysis. *Int. J. Pharm.* **42**:89–95 (1988).
2. M. E. Johansson and M. Nicklasson. Investigation of the film formulation of magnesium stearate by applying a flow-through dissolution technique. *J. Pharm. Pharmacol.* **38**:51–54 (1986).
3. L. R. Treupel and F. Puisieux. Distribution of magnesium stearate on the surface of lubricated particles. *Int. J. Pharm.* **31**:131–136 (1986).
4. Z. T. Chowhan and I. C. Yang. Powder flow studies IV. Tensile strength and flow rate relationships of binary mixture. *Int. J. Pharm.* **14**:231–242 (1983).
5. G. C. Lubner and G. Ricciardiello. Influence of flow promoting agents on the flow properties of mixtures of powders and on the physical properties of the resulting tablets. *Boll. Chim. Pharm.* **116**:40–52 (1977).
6. A. Otsuka. Adhesive properties and related phenomena for powdered pharmaceuticals. *Yakugaku Zasshi* **118**:127–142 (1998).
7. U. Sindel and I. Zimmermann. Measurement of interaction forces between individual powder particles using an atomic force microscope. *Powder Technol.* **117**:247–254 (2001).
8. S. Kondo, T. Ishikawa, and I. Abe. *Kyuchakunokagaku*, Maruzen, Tokyo, 1991.
9. Y. Shimada, Y. Yonezawa, H. Sunada, R. Nonaka, K. Katou, and H. Morishita. The development of an apparatus for measuring the adhesion force between fine particles. *J. Soc. Powder Technol. Jpn.* **37**:658–664 (2000).
10. S. Watano, T. Hamashita, and T. Suzuki. Removal of fine powders from film surface.I. Effect of electrostatic force on the removal efficiency. *Chem. Pharm. Bull.* **50**:1258–1261 (2002).
11. M. Mizuno, H. Sunada, K. Iida, A. Otsuka, H. Sakashita, H. Tada, and H. Kimura. Measurements of the adhesive force of fine particles on the tablet surfaces and its removal method. *Yakuzaigaku* **57**:181–189 (1997).
12. M. Fuji, K. Machida, T. Takei, T. Watanabe, and M. Chikazawa. Effect of surface geometric structure on the adhesion force between silica particles. *J. Phys. Chem. B.* **102**:8782–8787 (1998).
13. F. Podczeck, J. M. Newton, and M. B. James. The influence of constant and changing relative humidity of the air on the autoadhesion force between pharmaceutical powder particles. *Int. J. Pharm.* **145**:221–229 (1996).
14. M. Fuji, K. Machida, T. Takei, T. Watanabe, and M. Chikazawa. Effect of wettability on adhesion force between silica particles evaluated by atomic force microscopy measurement as a function of relative humidity. *Langmuir* **15**:4584–4589 (1999).
15. S. J. Gregg and K. S. W. Sing. *Adsorption, Surface Area and Porosity*, Academic Press, New York, 1982.
16. T. Oshima, Y. Zhang, M. Hirota, M. Suzuki, and T. Nakagawa. The effect of the types of mill on the flowability of ground powders. *J. Soc. Powder Technol. Jpn.* **30**:496–501 (1993).
17. H. Mizes, M. Ott, E. Ekulund, and D. Hays. Small particle adhesion: measurement and control. *Colloids Surfaces* **165**:11–23 (2000).
18. K. Cooper, A. Gupta, and S. Beaudoin. Substrate morphology

and particle adhesion in reacting systems. *J. Colloid Interface Sci.* **228**:213–219 (2000).
19. D. M. Schaefer, M. Carpenter, B. Gady, R. Reifenberger, L. P. DeMejo, and D. S. Rimai. *Fundamentals of Adhesion and Interfaces*, VSP, Utrecht, 1995.
20. Y. I. Rabinovich, J. J. Adler, A. Ata, R. K. Singh, and B. M. Moudgil. Adhesion between nanoscale rough surfaces II. Measurement and comparison with theory. *J. Colloid Interface Sci.* **232**:17–24 (2000).
21. E. R. Beach, G. W. Tormoen, J. Drelich, and R. Han. Pull-off force measurements between rough surfaces by atomic force microscopy. *J. Colloid Interface Sci.* **247**:84–99 (2002).
22. L. Sirghi, N Nakagiri, K. Sugisaki, H. Sugimura, and O. Takai, Effect of sample topography on adhesion force in atomic force spectroscopy measurements in air. *Langmuir* **16**:7796–7800 (2000).
23. J. Israelachvili. *Intermolecular and Surface Forces*, Academic Press, New York, 1992.
24. J. F. Pinto, G. Buckton, and J. M. Newton. A relationship between surface free energy and polarity data and some physical properties of spheroids. *Int. J. Pharm.* **118**:95–101 (1995).